DOE/BC/15319-2

High Resolution Prediction of Gas Injection Process Performance for Heterogeneous Reservoirs

Quarterly Report
July 1, 2002 to September 30, 2002

Contract No. DE-FC26-00BC15319

Principal Investigator: Franklin M. Orr, Jr.
Department of Petroleum Engineering
Stanford University

Disclaimer

Abstract

This report outlines progress in the fourth quarter of the second year of the DOE project "High Resolution Prediction of Gas Injection Process Performance for Heterogeneous Reservoirs".

In this report we document accomplishments in two areas of the current research project. First we describe results from an experimental study on the effects of interfacial tension (IFT) on three-phase relative permeabilities. Phase equilibrium measurements for a system containing water, hydrocarbon and two alcohols are reported. Furthermore, the effect of salinity on the three-phase regions is reported. Secondly we report on the progress related to incorporating gravity effects into compositional streamline simulation.

Contents

1. Executive Summary

A thorough understanding of the impact of various physical mechanisms is of significant importance to the successful design and implementation of enhanced oil recovery processes. In this report we describe the progress in two areas of importance to the development understanding of the fundamentals of multiphase flow and the representation of that flow in an accurate high-resolution compositional simulator.

First, we report the results of an ongoing experimental study on the impact of interfacial tension (IFT) on three-phase relative permeability. The significance of IFT variations within a reservoir subject to ternary recovery by gas injection or water alternating gas (WAG) processes has been observed but as of yet not analyzed in detail for three-phase systems. We report results of a study of water/hydrocarbon/alcohol(s)/NaCl systems that form three-phase as analogs to the gas/oil/water system found in reservoirs to avoid troublesome high-pressure experimental work. Detailed compositional analysis demonstrates how the IFT of three-phase mixtures of hexadecane/water/n-butanol can be controlled by gradually adding isopropanol or NaCl. The presented analog systems will be used in future flow experiments aiming to understand the interplay of IFT and three-phase relative permeability.

Second, the initial results of incorporating gravity effects in compositional streamline simulation by operator splitting are reported. For some production scenarios, e.g. gas condensate fields, effects of gravity may not be significant. However, for a large group of displacement problems, gravity segregation is an important mechanism. For these displacement problems sweep efficiency and local mixing of fluids must be predicted accurately by any simulator to match the processes occurring in the producing oil reservoir. A numerical approach for including gravity effects along gravity lines is described. Two example calculations are compared with a commercial simulator to demonstrate the accuracy of the suggested approach.

2. Impact of IFT on three-phase relative permeability

2.1 Introduction

Variation of interfacial tension (IFT) with temperature and pressure can have significant impact on displacement performance in miscible gas injection processes (Schechter *et al.*, 1994). Since gas injection process routinely includes three-phase flow (either because the reservoir has been previously waterflooded or because water is injected alternately with gas in order to improve overall reservoir sweep efficiency), the effect of IFT variations on three-phase relative permeabilities must be delineated if the performance of gas injection process is to be predicted accurately. In this study we present experimental results dealing with the first step of our systematic experimental program, in which the effect of IFT variation on the three-phase flow is being investigated.

Because they allow control of IFT in experiments performed at atmospheric pressure, oil/water/alcohol systems are useful for investigations of the effects of IFT variations. Here we consider the hexadecane (C_{16})/n-butyl alcohol (NBA)/H_2O system, which forms three liquid phases in equilibrium. The use of analog liquid phases serves many advantages in the laboratory determination of relative permeabilities: relatively low IFT reduces capillary end effects during displacement, IFT can be varied by changing the composition, and it is possible to create two phases that have low IFT in the presence of a third phase, just as gas/oil tensions can be low while oil/water and gas/water IFTs are not. A few researchers have already presented some applications for two-phase systems, isooctane (IC_8)/isopropyl alcohol (IPA)/brine (Morrow *et al.*,1988, Schechter *et al.,* 1994] and for three-phase systems, decane/benzyl alcohol/water [Grader and O'Meara, 1988]. IC_8 and brine forming two-phases were diluted by IPA until the IFT becomes zero. This is, of course, a good analogy to the miscible gas injection, in which the interfacial forces between the oil and gas phases become weaker, and eventually dismiss. The selection of reasonable liquid pairs with different IFT schemes for three-phase relative permeability measurements requires the knowledge of the phase behavior of appropriate components. Knickerbocker *et al.* (1982) presented the phase behavior of different hydrocarbon-alcohol-water combinations, which yield different three-liquid-phase patterns when salt is added. They studied all possible phase patterns for combinations of 10 monohydrid alcohols, 6 even-numbered n-alkanes having from 6 to 16, water with salinity from zero to 32 cg/mL.

The C_{16}/NBA/H_2O system gives appropriate phase behavior when IPA or NaCl is added to the mixtures. Adding either IPA or NaCl changes the compositions of the three equilibrium phases that form in a way that alters IFT appreciably. In the sections that follow we report results of phase composition, phase density, and IFT measurements.

2.2 Experimental Procedures

The chemicals used in the experiments were NBA (EM Science, 99.94%), C_{16} (Fisher Chemicals, 99.4%), IPA (Fisher Chemicals, 99.9%), IC_8 (Fisher Chemical, 99.4%) and NaCl (Baker, 99.6%). The aqueous phase was distilled, de-ionized H_2O.

All experiments were performed at room temperature, 22±0.4 °C. All components were mixed in the 60-cc glass vials based on their weights taken with the balance with 0.001g reproducibility. After shaking the mixtures by hand the equilibrated phases separated in times that ranged from minutes to one day.

The equilibrated phases were sampled by syringe and transported to 1.5-cc vials for gas chromatography measurements. To prevent contamination by the phases above when sampling lower and middle phases, a small amount of air withdrawn by syringe before sampling was pushed out in the correspondent phase to clean any contamination at the edge of the needle. Liquid phase compositions were analyzed with a Hewlett-Packard 5880A temperature programmable gas chromatography. Satisfactory separations were obtained by using the 6’x1/8”x0.085” stainless steel column packed with 10%Carbowax 20M on 80/100 Chromosorb W-HP (Alltech Associates). The peaks for the components, C_{16}, NBA, IPA, and H_2O, were calibrated with mixtures containing known amounts of the components.

The IFTs between the phases were measured with a spinning drop tensiometer manufactured by University of Texas (Model 300), which is very reliable for low IFTs. The tensiometer was calibrated by known IFT values of tie lines on the phase diagram of IC8/2%$CaCl_2$ H_2O/IPA system presented by Morrow *et al.* (1988).

The densities were measured by using a 10-cc Gay-Lussac bottle based on gravity method. Chloride concentrations were determined by sampling each phase and evaporating the liquid components at elevated temperatures.

2.3 Experimental Results and Interpretation

The effects of increasing IPA fraction or of increasing NaCl concentration were examined for C_{16}/NBA/H_2O mixtures that formed three phases. First of all, the base ternary phase diagram for C_{16}/NBA/H_2O system was obtained (Mix 1 on Figs. 1 and 2 and Tables 1 and 2). A large three-phase region surrounded by two-phase regions was observed for the ternary system (Fig.1). Each of the edges of the three-phase region is also a tie line for an associated two-phase region. The fact that all binary mixtures of C_{16} and NBA are completely miscible at 22 °C indicates that the two-phase region connected to the tie line of three-phase region between C_{16}-rich and NBA-rich phases must lie inside the ternary triangle that forms the bottom of the quaternary diagram (Fig.1). The C_{16}-rich upper phase (82%) contains only a small amount of H_2O (approx. 1.5%). The NBA-rich middle phase (75%) has 13% H_2O and 12% C_{16}. A very low fraction of C_{16} (approx.

0.3%) was detected in the lower aqueous phase which contains 15% NBA. Based on this ternary liquid system, we added gradually IPA or NaCl to obtain a sequence of tie triangles shown in the quaternary phase diagrams.

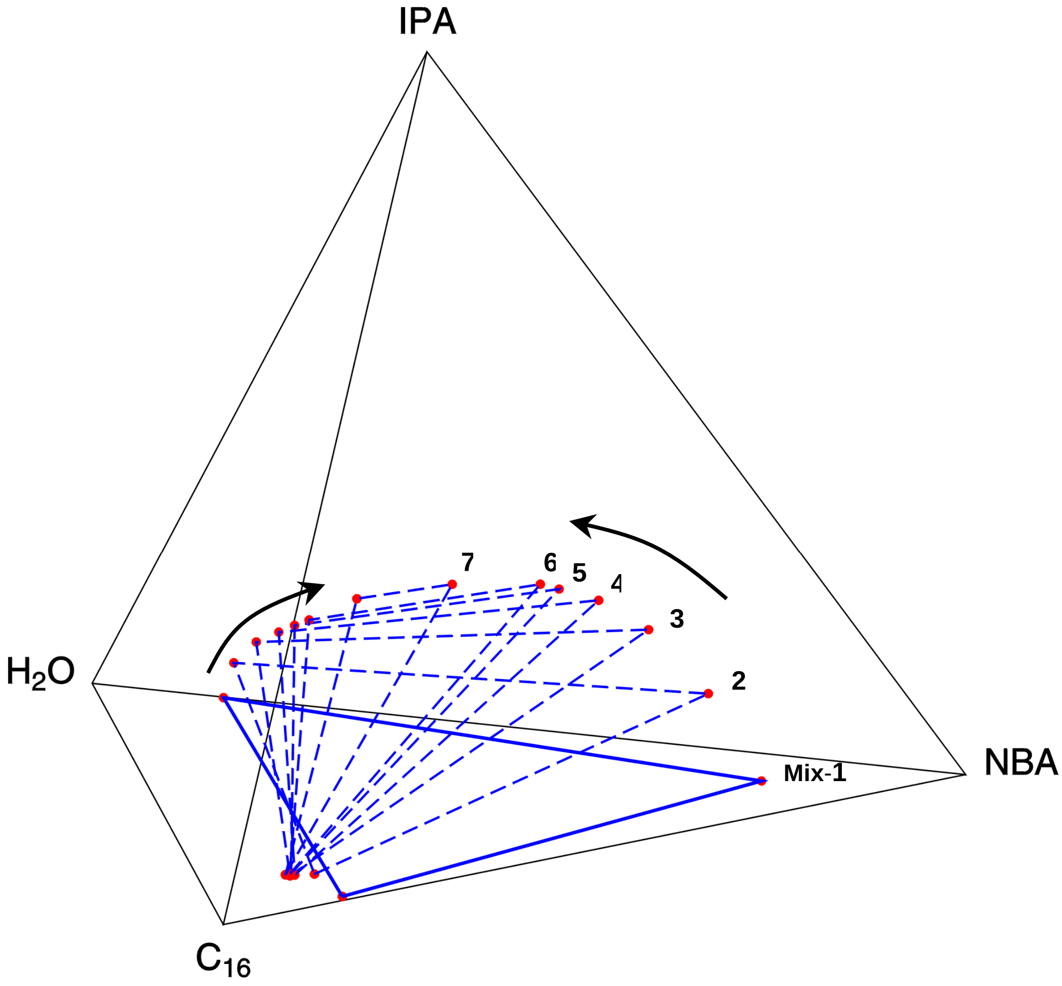

Fig. 1: Tie triangles for the hexadecane/n-butanol/isopropanol/water system.

Fig. 1 shows the quaternary phase diagram obtained by increasing the IPA fraction in the mixture. As IPA concentration was increased, the IFT between lower and middle phases decreased (Table 1). With the same increase in the IPA ratio the IFT between upper and middle phases is getting higher, whereas the IFT between upper and lower phases stay almost constant. When the IFT between lower and middle phases reaches a zero, the other two IFTs become identical, which means that only two phases exist in the system. For three-phase flow experiments, we can choose the H_2O-rich phase to represent the oil phase, the NBA-rich phase to represent the gas phase, and the C_{16}-rich phase to represent the aqueous phase. Because IPA is relatively volatile, care will be required in displacement experiments to avoid composition changes caused by evaporation.

The quaternary phase diagram for C_{16}/NBA/H_2O/NaCl is shown in Fig. 2. As salt is added to the mixture, most of the salt goes to the aqueous phase and increasing salt concentration drives alcohol out of the aqueous phase. Because NBA and C_{16} are completely miscible in all proportions the upper and middle phases are going to have a trend to be miscible. Thus, the IFT between upper and lower phases is getting lower whereas the other two IFTs are almost identical (Table 2). As an analogy to three-phase fluid systems in gas injection, the C_{16}-rich phase can be used to represent as the gas phase, the NBA-rich phase to represent the oil phase, and the H_2O-rich phase to represent the aqueous phase.

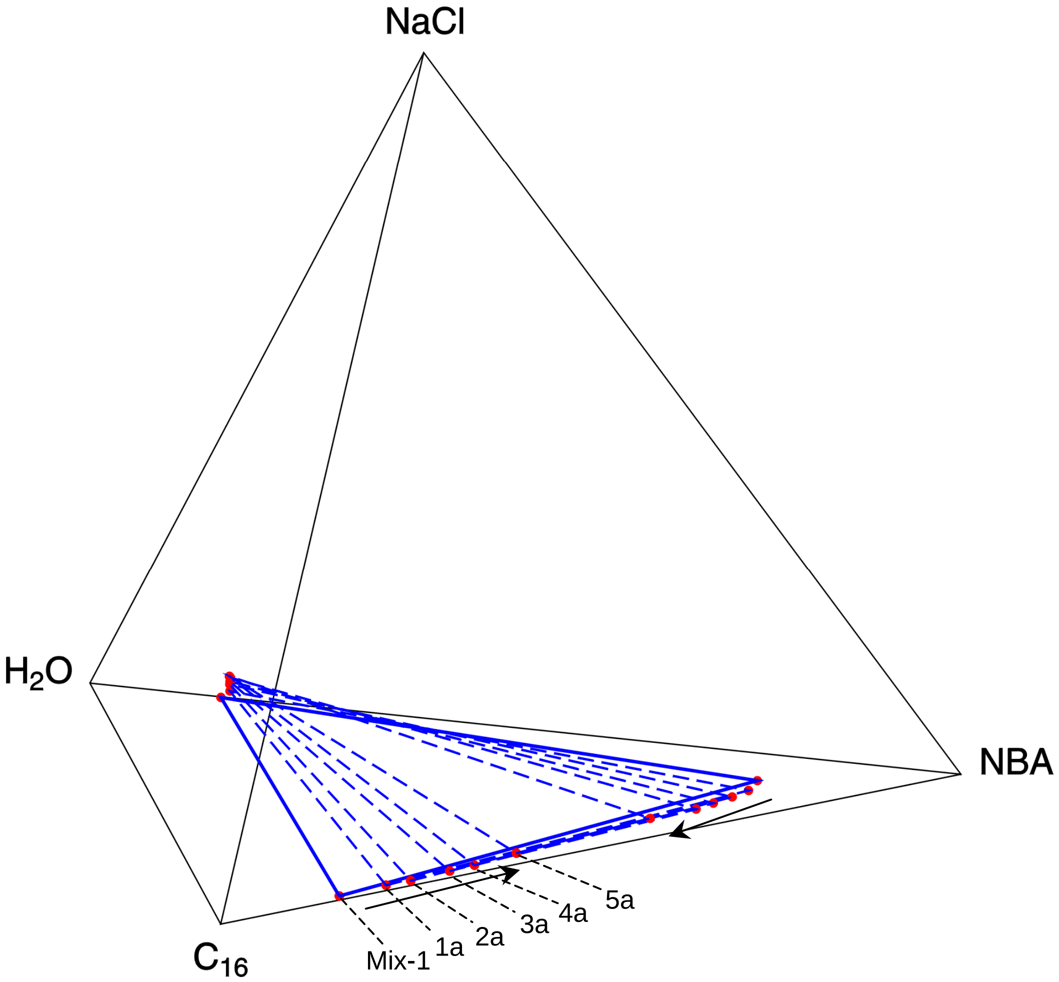

Fig. 2: Tie triangles for the hexadecane/n-butanol/water/NaCl system.

The two systems presented offer some flexibility in the design of displacement experiments to investigate effects of IFT variations in three-phase flow. For example, injection of pre-equilibrated three-phase systems should allow control of IFT between pairs of phases with low IFT between one pair. Designs of those experiments will be discussed in future reports.

Table 1 – Composition, density, and IFT for Fig.1.

Samples		Mix. 1	Mix. 2	Mix. 3	Mix. 4	Mix. 5	Mix. 6	Mix. 7
Overall IPA, %		0	4.5	9.1	11	12.51	15.05	15.09
(U)pper Phase	C_{16}	0.822	0.836	0.866	0.858	0.855	0.858	0.864
	NBA	0.163	0.116	0.082	0.089	0.085	0.083	0.077
	H_2O	0.015	0.014	0.014	0.016	0.022	0.021	0.021
	IPA	0.000	0.034	0.038	0.037	0.038	0.038	0.038
	ρ, g/cm^3	0.776	0.774	0.774	0.772	0.773	0.772	0.773
(M)iddle Phase	C_{16}	0.122	0.076	0.042	0.024	0.019	0.015	0.006
	NBA	0.748	0.653	0.561	0.495	0.447	0.425	0.332
	H_2O	0.130	0.164	0.215	0.269	0.313	0.336	0.455
	IPA	0.000	0.107	0.182	0.212	0.221	0.224	0.207
	ρ, g/cm^3	0.824	0.837	0.846	0.858	0.866	0.870	0.903
(L)ower Phase	C_{16}	0.003	0.003	0.001	0.000	0.001	0.000	0.002
	NBA	0.150	0.141	0.154	0.173	0.186	0.199	0.238
	H_2O	0.847	0.802	0.757	0.721	0.694	0.672	0.591
	IPA	0.000	0.054	0.088	0.106	0.119	0.129	0.169
	ρ, g/cm^3	0.987	0.983	0.976	0.969	0.964	0.960	0.946
IFT, dyne/cm	U/L	2.465	2.068	1.893	1.850	1.801	1.749	1.583
	U/M	0.239	0.551	0.794	1.106	1.166	1.491	1.622
	M/L	2.297	1.157	0.654	0.308	0.162	0.086	0.028

Table 2 – Composition, density, and IFT for Fig.2.

Samples		Mix. 1	Mix. 1a	Mix. 2a	Mix. 3a	Mix. 4a	Mix. 5a
Overall NaCl, %		0	1.17	2.33	2.89	3.45	3.54
(U)pper Phase	C_{16}	0.822	0.753	0.722	0.664	0.627	0.555
	NBA	0.163	0.227	0.260	0.313	0.347	0.406
	H_2O	0.015	0.020	0.018	0.022	0.025	0.038
	NaCl	0.000	0.000	0.000	0.001	0.001	0.001
	ρ, g/cm^3	0.776	0.776	0.780	0.784	0.783	0.786
(M)iddle Phase	C_{16}	0.122	0.172	0.211	0.247	0.281	0.343
	NBA	0.748	0.730	0.705	0.678	0.653	0.591
	H_2O	0.130	0.097	0.082	0.073	0.064	0.064
	NaCl	0.000	0.001	0.002	0.002	0.002	0.002
	ρ, g/cm^3	0.824	0.816	0.810	0.809	0.803	0.798
(L)ower Phase	C_{16}	0.003	0.000	0.000	0.002	0.000	0.000
	NBA	0.150	0.157	0.153	0.151	0.150	0.148
	H_2O	0.847	0.833	0.827	0.822	0.820	0.820
	NaCl	0.000	0.010	0.021	0.025	0.030	0.032
	ρ, g/cm^3	0.987	1.022	1.043	1.055	1.066	1.067
IFT, dyne/cm	U/L	2.465	3.244	4.265	4.267	4.714	4.645
	U/M	0.239	0.083	0.038	0.012	0.005	0.001
	M/L	2.297	3.187	3.824	4.182	4.772	4.179

2.4 Conclusions

Two four-component three-liquid-phase quaternary phase diagrams have been determined that will allow investigation of the effects of IFT variation on three-phase flow. The phase diagrams demonstrate that three-phase systems can be created that exhibit low IFT between one pair of phases, a situation that is analogous to that created in multicontact miscible gas injection processes with water present.

3. Gravity and Compositional Streamline Simulation

3.1 Introduction

In a previous quarterly report, we presented the preliminary results from combining analytical 1D solutions to gas injection problems with streamline simulation. Those simulations were restricted to production scenarios where gravity effects are of minor importance. In this section we focus on removing that restriction through incorporation of gravity effects by operator splitting.

3.2 Mathematical Model

In this section we derive the mass conservation equations for multicomponent multiphase flow with emphasis on including gravity segregation in compositional streamline simulation. Mass conservation of n_c components distributed in n_p phases, flowing through a heterogeneous porous medium can be stated as[5]

$$\phi \frac{\partial}{\partial t}\left\{\sum_{j=1}^{n_p} \omega_{ij}\rho_{mj}S_j\right\} + \nabla\left\{\sum_{j=1}^{n_p} \omega_{ij}\rho_{mj}\underline{u}_j\right\} = 0\,, \quad i = 1,..,n_c\,, \tag{1}$$

where ϕ is the porosity, t is the time, ω_{ij} is the mass fraction of component i in phase j, ρ_{mj} is the mass density of phase j, S_j is the gas saturation and u_j is the velocity of phase j. According to Darcy's law, the velocity of phase j can be written in terms of the total permeability ($\underline{\underline{K}}$), the relative permeability of phase j (k_{rj}), the viscosity (μ_j) and the mass density of phase j

$$\underline{u}_j = -\frac{\underline{\underline{K}}k_{rj}}{\mu_j}\left(\nabla P + \rho_{mj} g \nabla D\right),\ \ j = 1,..,n_p\,, \tag{2}$$

where P, D and g are the pressure, depth and gravity. For flow problems that are strongly coupled to the phase behavior of the flowing phases, it is more convenient to work with the conservation equations stated in terms of mole fractions and molar densities;

$$\phi \frac{\partial}{\partial t}\{C_i\} + \nabla\left\{\sum_{j=1}^{n_p} x_{ij}\rho_j \underline{u}_j\right\} = 0\,, \quad i = 1,..,n_c\,, \tag{3}$$

with

$$C_i = \sum_{j=1}^{n_p} x_{ij}\rho_j S_j\,, \quad i = 1,..,n_c \tag{4}$$

where x_{ij} is the mole fraction of component *i* in phase *j* and ρ_j is the molar density of phase *j*.

With focus on the effects of gravity (i.e. flow in the vertical direction) we assume that the total velocity in a gas/oil displacement problem is approximated accurately by assuming incompressible flow. For incompressible flow, the total velocity ($\underline{u}_t$) can be written as

$$\underline{u}_t = -\underline{\underline{K}}\left(\lambda_t \nabla P + \lambda_g \nabla D\right) = \sum_{j=1}^{n_p} \underline{u}_j\,, \tag{5}$$

with the total mobility (λ_t) and the total gravity mobility (λ_g) given by

$$\lambda_t = \sum_{j=1}^{n_p} \lambda_j = \sum_{j=1}^{n_p} \frac{k_{rj}}{\mu_j} \quad \text{and} \quad \lambda_g = g\sum_{j=1}^{n_p} \lambda_j \rho_{mj} \tag{6}$$

Upon substitution of the Darcy velocity into Eq. 3, the conservation equations can be rewritten along a gravity line (vertical line) as

$$\phi \frac{\partial}{\partial t}\{C_i\} - \frac{\partial}{\partial z}\left\{\sum_{j=1}^{n_p} x_{ij}\rho_j K_z \lambda_j \left(\frac{\partial P}{\partial z} + \rho_{mj} g \frac{\partial D}{\partial z}\right)\right\} = 0\,, \quad i = 1,..,n_c \tag{7}$$

The gradient in pressure can be eliminated from Eq. 7 by Eq. 5 rewritten as

$$\frac{\partial P}{\partial z} = -\frac{u_z}{K_z \lambda_t} - \frac{\lambda_g}{\lambda_t}\frac{\partial D}{\partial z} \tag{8}$$

Finally, by substitution of Eq. 8 into Eq. 7 we obtain

$$\phi \frac{\partial}{\partial t}\{C_i\} + \frac{\partial}{\partial z}\{F_i\} + \frac{\partial}{\partial z}\{G_i\} = 0\,, \quad i = 1,..,n_c \tag{9}$$

where F_i is the vertical convective flux of component *i* given by

$$F_i = u_z \sum_{j=1}^{n_p} x_{ij} \rho_j f_j \ , \quad i = 1,..,n_c \, , \tag{10}$$

and G_i is the gravity flux of component *i* given by

$$G_i = K_z \sum_{j=1}^{n_p} x_{ij} \rho_j \lambda_j \left(\frac{\lambda_g}{\lambda_t} - \rho_{mj} g \right) \frac{\partial D}{\partial z} \ , \quad i = 1,..,n_c \tag{11}$$

In black-oil/immiscible streamline simulation Eq. 9 is commonly solved in a sequentially manner by operator splitting[6-9]. Operator splitting relies on the consistency of treating the convective flux independently from the gravity flux within a given time step of the simulation. In other words, any given time step starts with a convective step solving

$$\phi \frac{\partial}{\partial t} \{ C_i \} + \frac{\partial}{\partial z} \{ F_i \} = 0 \ , \quad i = 1,..,n_c \, , \tag{12}$$

followed by a gravity step solving

$$\phi \frac{\partial}{\partial t} \{ C_i \} + \frac{\partial}{\partial z} \{ G_i \} = 0 \ , \quad i = 1,..,n_c \tag{13}$$

In the following section we address the problem of solving the gravity equation (Eq. 13) for compositional problems.

3.3 Numerical Scheme

To solve the gravity equation (Eq. 13) for a give time interval, we must apply a numerical scheme, as no analytical solutions are available. We rewrite the gravity equation in the general discrete form

$$C_{i,k}^{n+1} = C_{i,k}^{n} - \frac{\Delta t}{\Delta z} \left\{ G_{i,k+1/2}^{n} - G_{i,k-1/2}^{n} \right\} = 0 \ , \quad i = 1,..,n_c \, , \tag{14}$$

where *i*, *k* and *n* refer to component *i* in grid block *k* at time step *n*. The gravity flux at the block interfaces *k+1/2* and *k-1/2* must be chosen carefully bound by the direction of motion of the individual phases. In the current study we restrict the analysis to two-phase gas/oil flow problems. Fig. 3 demonstrates the appropriate discretization of a 1D vertical gas/oil problem. For any grid block containing two phases in equilibrium, the gas is assumed to be lighter than the oil and hence move upwards.

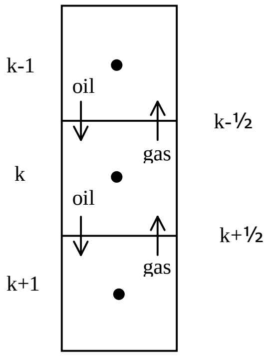

Fig. 3: Discretization of a 1D vertical gas/oil problem.

At the interface *k+1/2* in Fig.3, we note that the upwind direction for a gas phase is *k+1* whereas the upwind direction for an oil phase is *k*. Given these upwind directions the gravity flux at *k+1/2* is given by

$$G^n_{i,k+1/2} = g\frac{\partial D}{\partial z}\left\{\beta_{\mathrm{i,k+1/2}}\left(\alpha_{k+1/2} - \rho_{mx,k}\right) + \gamma_{i,k+1/2}\left(\alpha_{k+1/2} - \rho_{my,k+1}\right)\right\},\quad i = 1,..,n_c \tag{15}$$

where

$$\alpha_{k+1/2} = \frac{\left(K_z\lambda_x\rho_{mx}\right)_k + \left(K_z\lambda_y\rho_{my}\right)_{k+1}}{\left(K_z\lambda_x\right)_k + \left(K_z\lambda_y\right)_{k+1}} \tag{16}$$

$$\beta_{\mathrm{i,k+1/2}} = \left(\mathrm{x_i}\rho_x \mathrm{K_z}\lambda_x\right)_{\mathrm{k}},\quad i = 1,..,n_c \tag{17}$$

$$\gamma_{\mathrm{i,k+1/2}} = \left(\mathrm{y_i}\rho_y \mathrm{K_z}\lambda_y\right)_{\mathrm{k+1}},\quad i = 1,..,n_c \tag{18}$$

In Eqs. (15-18), subscripts x and y denote the liquid and vapor phase respectively. x_i and y_i are the mole fractions of component *i* in the liquid and vapor phases.

3.4 Preliminary Test Results

To test the numerical scheme outlined in Section 3.3, we consider a simple quaternary mixture consisting of N_2, C_1, C_4 and C_{10} in equal amounts (mole basis) at 344K. The phase behavior of the mixture was modeled by the Peng-Robinson equation of state whereas the viscosity was predicted by the Lohrenz-Bray-Clark correlation[10]. A homogeneous 20m column with a permeability of 500 mD was initially studied. Cory-type relative permeability functions are specified with a $S_{or} = 0.2$. The total hydrostatic pressure gradient along this column was approximately 1 atm and hence relatively insignificant compared to the pressure of 100 atm specified at the top. At 100 atm the mixture forms two phases and the system was initialized with two phases throughout the entire column. The vapor and liquid phases was then allowed to move according to their individual gravity potential until a steady state was reached. Figs. 4 and 5 show a comparison of the final state (reached after approximately 100 days of simulation) in terms of saturation and concentration profiles obtained by the scheme of Sec. 3.3 and the commercial simulator Eclipse 300.

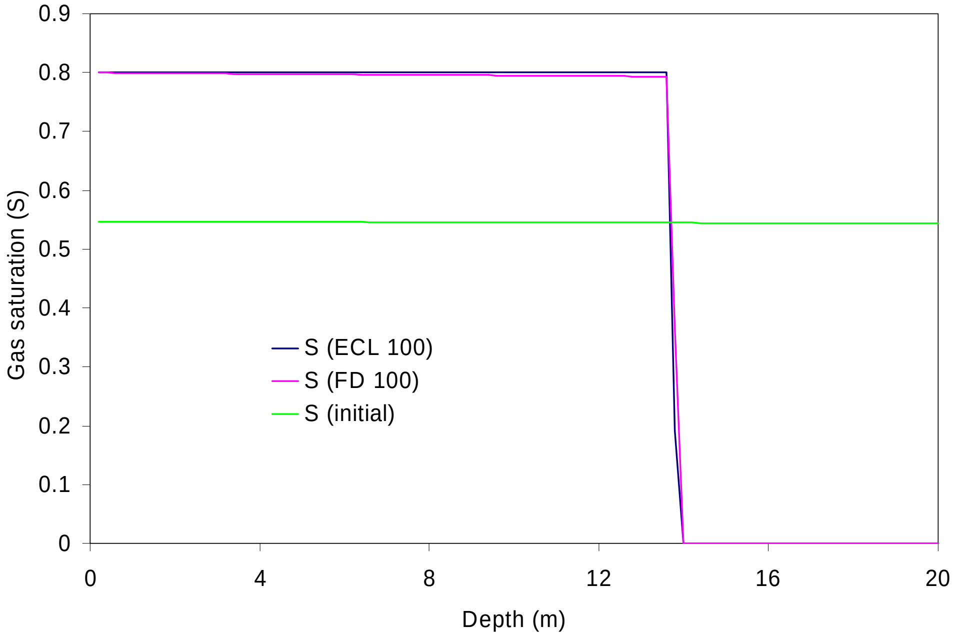

Fig. 4: Gas saturation profiles at initial and steady state. Comparison of Eclipse 300 (E300) and the numerical scheme outlined in Sec. 3.3. 100 grid blocks were used for both simulations.

Figs. 4 and 5 show excellent agreement between the suggested finite difference (FD) scheme and E300 although the FD scheme appears to be slightly more diffusive around the gas-oil contact.

A second test problem was designed to test the performance of the numerical scheme for cases with impermeable barriers. The two center blocks were assigned zero permeability to imitate a shale layer in a reservoir formation. The results of the second test problem in terms of steady state saturation profiles are reported in Fig. 6. As for the first example calculation, excellent agreement is found between the two methods.

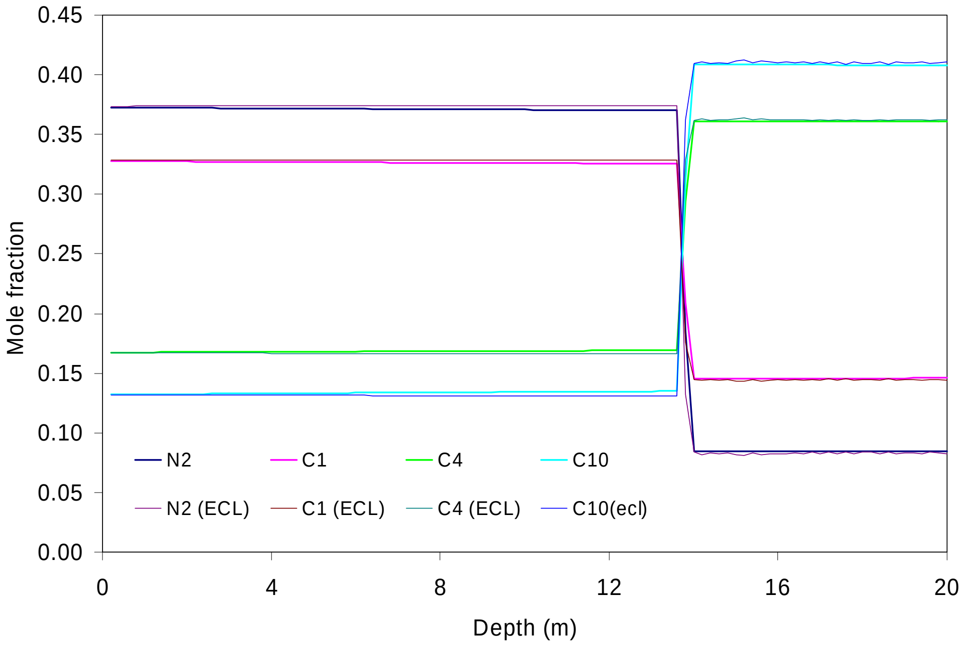

Fig. 5: Concentration profiles at steady state. Comparison of Eclipse 300 (E300) and the numerical scheme outlined in Sec. 3.3. 100 grid blocks were used for both simulations.

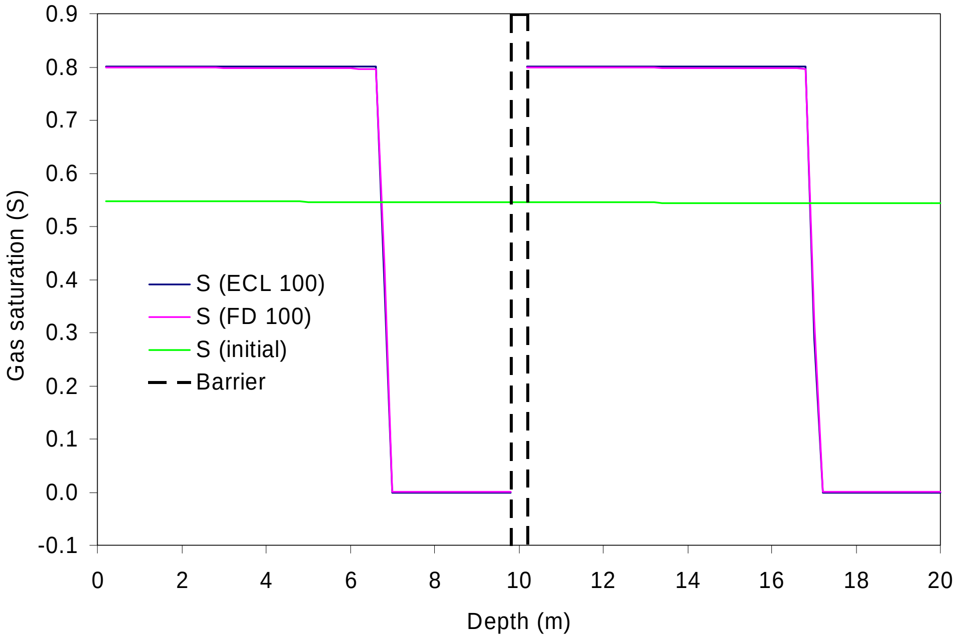

Fig. 6: Comparison of saturation profiles predicted for a layered column at steady state, generated by FD and E300.

3.5 Conclusions

In the previous sections, the mathematical framework for incorporating effects of gravity into a compositional streamline simulator has been outlined. A numerical scheme for solving the resulting system of PDE's has been presented and tested in two simple example calculations. Excellent agreement with the commercial simulator E300 was found. Further testing of the suggested approach will be carried out in the near future prior to the implementation of the gravity step into the streamline simulator developed by SUPRI-C at Stanford University.

4. References

1. Knickerbocker, B.M., Peskeck, C.V., Davis, H.T., and L.E. Scriven: Patterns of three-liquid-phase behavior illustrated by alcohol-hydrocarbon-water-salt mixtures. J. Phys. Chem., 86, p.393-400, 1982.
2. Grader, A.S. and O'Meara, D.J.: Dynamic displacement measurements of three-phase relative permeabilities using three immiscible liquids. SPE 18293, presented at the SPE 63rd Ann. Tech. Conf. and Exhib., Houstan, TX, Oct. 2-5, 1988.
3. Morrow, N.R., Chatzis, I., and Teber, J.J.: Entrapment and mobilization of residual oil in bead packs. SPE 14423, SPE Reservoir Engineering, p.927-935, August 1988.
4. Schechter, D.S., Zhou, D., and Orr, F.M., Jr.: Low IFT drainage and imbibition. J. of Pet. Sci. and Eng., 11, p.283-300, 1994.
5. Lake, L.W.: "Enhanced Oil Recovery", Prentice Hall Publishers, New York City (1989), p. 29.
6. Bradtvedt, F., Gimse, T. and Tegnander, C.: "Streamline computations for porous media flow including gravity", Transport in Porous Media, 1996, Vol. 25, No. 1, 63-78.
7. Bradtvedt, F., Bradtvedt, K., Buchholz, C., Holden, L.,Holden, H., and Risebro, N.H. "A New Front-Tracking Method for Reservoir Simulation", SPE Reservoir Engineering, Feb. 1992, 107-116.
8. Batycky, R.P. *A Three-Dimensional Two-Phase Field Scale Streamline Simulator*, Ph.D. thesis, Stanford University, Stanford, CA, 1992.
9. Batycky, R.P., Blunt, M.J., and Thiele, M.R.: "A 3D Field Scale Streamline Simulator with Gravity and Changing Well Conditions", SPE 36726, Proceedings of the 1996 SPE ATCE, Denver, CO, Oct. 6-9.
10. Lohrenz, J., Bray, B.G., and Clark, C.R.: "Calculating Viscosities of Reservoir Fluids From Their Compositions," *JPT* (October 1964) 1171.